IEEE Access
Multidisciplinary | Rapid Review | Open Access Journal

Received June 28, 2020, accepted August 6, 2020, date of publication August 11, 2020, date of current version August 21, 2020.

Digital Object Identifier 10.1109/ACCESS.2020.3015839

Three Adaptive Sub-Histograms Equalization Algorithm for Maritime Image Enhancement

CHANG DING[1], XIPENG PAN[2], XINGYU GAO[1], LIHUA NING[3], AND ZIKU WU[4]

[1]School of Mechanical and Electrical Engineering, Guilin University of Electronic Technology, Guilin 541004, China
[2]School of Computer and Science and Information Security, Guilin University of Electronic Technology, Guilin 541004, China
[3]School of Mathematics and Computing Science, Guilin University of Electronic Technology, Guilin 541004, China
[4]School of Science and Information, Qingdao Agricultural University, Qingdao 266109, China

Corresponding author: Lihua Ning (nlhua@sina.com)

This work was supported in part by the Innovation Driven Development Special Fund Project of Guangxi under Grant AA18118002-3, and in part by the Project of Foundational Research Ability's Improvement for Young and Middle-aged Teachers of University in Guangxi under Grant 2020KY05019 and Grant 2020KY05034.

ABSTRACT According to maritime image histograms' statistic and analysis, the histogram of pure maritime image obeys Gaussian distribution approximately, thus Three Adaptive Sub-histograms Equalization (TASHE) algorithm for maritime image enhancement is proposed in this paper. First, the characteristics of pure maritime image's histogram are studied, then the adaptive threshold's optimal selection strategy for the histogram's division is discussed, finally the implement of three sub-histograms is described. This paper employs visible gray maritime image, visible color maritime image and infrared maritime image to verify the enhancement algorithm's effectiveness and robustness, the experimental results show that TASHE algorithm can not only keep the maritime image's mean brightness and naturalness, but also improve the maritime image's contrast without the noise and artifacts. The objective image quality assessment also indicates that TASHE algorithm can improve the original maritime image's Enhancement Measure by Entropy (EME) value, furthermore, when a maritime image is pre-processed by TASHE algorithm, the maritime target's Detection Rate (DR) can be improved.

INDEX TERMS Image enhancement, sub-histogram equalization, maritime image, Gaussian distribution.

I. INTRODUCTION

Histogram Equalization (HE) [1] is one of the most widely used methods in image enhancement [2]–[5], which has the advantages of easy computation and implementation [6]. Nevertheless, the result after histogram equalization brings about some disadvantages [7] such as mean gray value's fixing, entropy's declination, and the details' missing. Aiming at the disadvantages of HE, some representative improved methods are proposed.

Some researchers study the sub-histogram equalization methods, which can enhance the image and prevent the over-enhancement, for example, Brightness Preserving Bi-Histogram Equalization (BBHE) [8] first divides the image histogram into two parts(sub-histograms), and then the two sub-histograms are independently equalized, which can preserve the original image's mean brightness. Equal Area Dualistic Sub-Image Histogram Equalization (DSIHE) [9] divides the histogram into two sub-histograms based on its original probability density function, which can obtain the maximum entropy. Minimum Mean-Brightness Error Bi-Histogram Equalization (MMBEBHE) [10] is the extension of BBHE, which provides maximal brightness preservation. In Jan. 2020, Khan *et al.* [7] proposed the method of fuzzy bi-histogram equalization, the key technique of this method is that the histogram's dividing threshold can be derived from the skewness of the histogram, which indicates that the threshold of sub-histogram equalization can be selected by the characteristic of the image's histogram. Some researchers have also studied the modified histogram equalization methods named by weighted histogram technique, thresholded histogram technique, or clipped histogram technique, finally histogram equalization operates the new histogram, the enhancement result usually has a better performance, this is because the pixel's frequency of histogram can control the image's enhancement rate. For example,

The associate editor coordinating the review of this manuscript and approving it for publication was You Yang.

Weighted Thresholded Histogram Equalization (WTHE) [11] limits and modifies the original image's histogram by a transformation function, the enhancement result can reduce the over-enhancement. Bi-Histogram Equalization with a Plateau Limit (BHEPL) [12] controls the enhancement's degree by limiting the gray value's frequency, the enhancement result can keep the original image's brightness. In the reformed process of HE technique, image's characteristics can also be used as the dividing threshold, for example, exposure based Sub Image Histogram Equalization (ESIHE) [13] combines the idea of BBHE and BHEPL, which takes the image's exposure as the threshold to divide the histogram into two sub-histograms, then the two sub-histograms are clipped by the other threshold, finally the two novel sub-histograms are equalized respectively, the ESIHE algorithm is suitable for enhancing the low exposure gray image. The Recursively Separated and Weighted Histogram Equalization (RSWHE) [14] divides the entire histogram into the sub-histogram recursively, and the High-speed Quantile-based Histogram Equalization (HSQHE) [15] divides the entire histogram by quantile values, both of two algorithm may be not effective when enhancing the maritime image, because the principle of two algorithms doesn't consider the characteristics of the histogram of maritime image. To enhance the image's local details, some researchers improved the idea of HE in the histogram of an image's local area. For example, Partially Overlapped Sub-block Histogram Equalization (POSHE) [16] and Local Histogram Equalization (LHE) [17] use a small window that slides through every image pixel sequentially, and only pixels within the current position of the window are histogram equalized, both of the two algorithms take local information into consideration when enhancing the image, which can enhance the image's details obviously, but over-enhancement are sometimes occurred. The idea of HE can also be used in the Discrete Wavelet Domain (DWT) [18], when the original image is decomposed into low-frequency and high-frequency components by DWT, the low-frequency coefficients' histograms are equalized, the high-frequency coefficients are kept constant and the reconstructed image can be obtained, finally weighting the original image and the reconstructed image can get the better performance's result. Some researchers propose a new histogram's definition and concept which can better reflect the image's variation information, for example, Singh *et al.* [19] considered that the rough region of the image can reflect the image's feature information more effectively, so a novel histogram can be derived from the image's rough region, then the entire image's mapping function can be calculated by the novel histogram equalization, in his work, two algorithms named by Dominant Orientation-based Texture Histogram Equalization (DOTHE) and Edge-based Texture Histogram Equalization (ETHE) are proposed. However, if a maritime image appears some small targets, in such case, the small target's region cannot reflect the image's feature information effectively, so the enhancement result often has some artifacts when DOTHE and ETHE algorithms are used to enhance the maritime image. In the study of image enhancement of sea water, Song *et al.* [20] established a variational model for enhancing the maritime image without any maritime target, but as for a maritime image including a maritime target, Song's algorithm may not be enough effective and has less help in the maritime target's tracking and recognition. In our work, we consider the characteristics of maritime image's histogram, optimize and improve the idea of the sub-histogram equalization, the design of our algorithm is equalizing the three sub-histograms by two adaptive thresholds to enhance the maritime image, and then TASHE algorithm is proposed in this paper.

The remainder of this paper is organized as follows: Section II introduces the characteristics of the maritime image's histogram, Section III discusses the adaptive threshold's selection derived from the original image's histogram and the optimal strategy of threshold selection, Section IV describes the implement of TASHE algorithm, Section V shows the experimental results and assesses the enhancement result's objective quality of each algorithm, and Section VI concludes the paper.

II. RESEARCH ON THE CHARACTERISTICS OF MARITIME IMAGE'S HISTOGRAM

A. RESEARCH ON THE CURVE'S VARIATION OF MARITIME IMAGE'S HISTOGRAM

In order to explain the characteristics of maritime image's histogram and make some investigations and demonstrations sufficiently, four visible gray maritime images, four visible color maritime images and four infrared maritime images are shown as an illustration in Fig.1, and all of the maritime images contain the pure sea background and include some small maritime targets such as boat, yacht and surfer.

Mean filter with the size of 1×13 is used to denoise the original histogram in order to make the histogram's curve smooth, which can be observed more clearly, the filtered histograms of the above-mentioned maritime images are shown in Fig.2, as for Fig.2(b), we show the V component's histogram in HSV color space, from which, it can be summarized that the histogram curve of each maritime image rises firstly and then arrives at a peak value, finally the curve declines near to zero. According to the curves' variation tendency, it can also be seen that the histogram of a maritime image obeys the Gaussian distribution nearly.

On the study of image histogram's fitting, Celik *et al* [21]. use the Gaussian Mixture Model (GMM) to model the image's histogram, if an image can be decomposed into the background region and target region, two-order GMM can fit the image's histogram in the common case. According to Celik's work [21], as for a maritime image with pure sea background, the sea background is large, but the maritime target's region is small, which can be ignored, thus one-order Gaussian distribution can fit a maritime image's histogram instead of GMM. In the following, Gaussian distribution is used to fit the maritime image's histogram with estimated parameters by Maximum Likelihood Estimate (MLE) law [22].

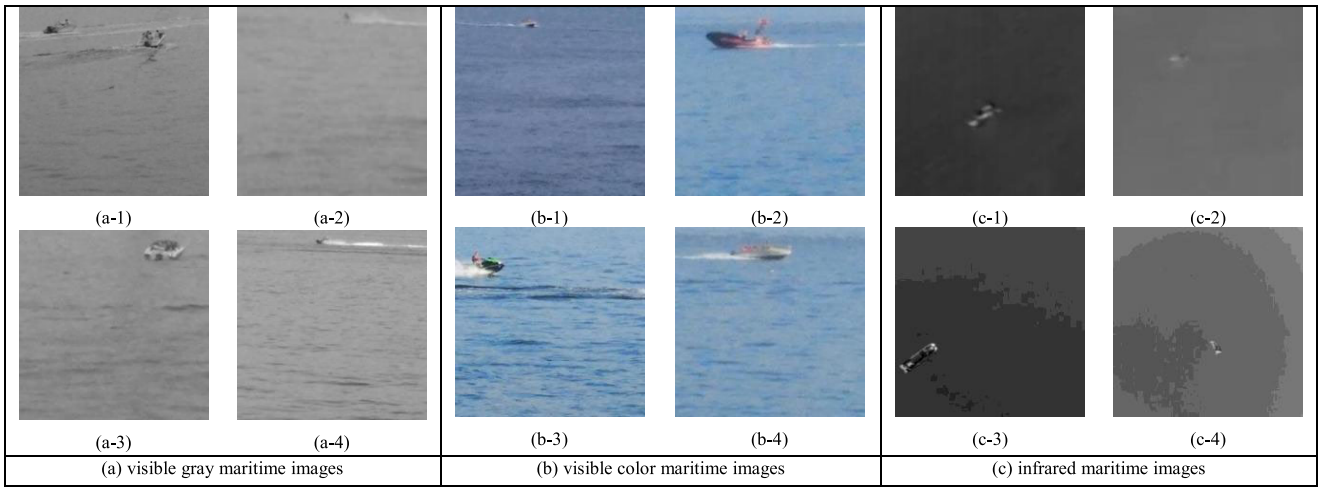

FIGURE 1. Four visible maritime images, four gray maritime images and four infrared maritime images.

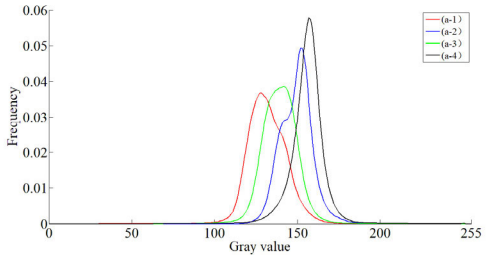

(a) The histograms' curve of Fig.1(a)

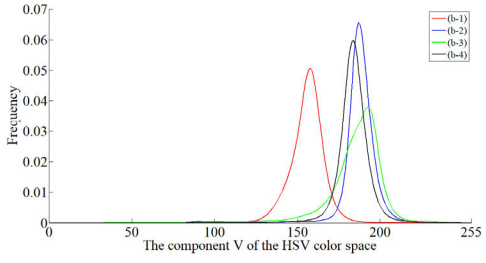

(b) The histograms' curve of Fig.1(b)

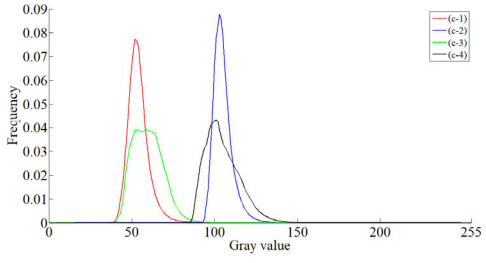

(c) The histograms' curve of Fig.1(c)

FIGURE 2. The filtered histograms' curve of three kinds of maritime images.

B. PARAMETER ESTIMATION AND SIMILARITY ASSESSMENT

Now, we use Fig.3(a) (enlarged by Fig.1(b)) as a illustration to explain how to use Gaussian distribution to fit a maritime image's histogram, the experimental maritime image's actual histogram and Gaussian distribution's fitting curve are shown in Fig.3(b).

(a) The maritime image with two targets

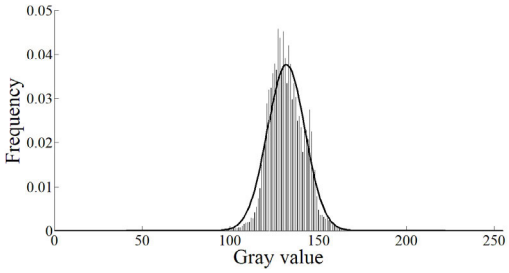

(b) Actual histogram bar and the fitting curve

FIGURE 3. Experimental image's actual histogram and Gaussian distribution's fitting curve.

According to MLE law, $\hat{\mu}$ and $\hat{\sigma}$ in Gaussian distribution can be estimated respectively according to (1).

$$\hat{\mu} = \bar{x}, \quad \hat{\sigma} = \sqrt{\frac{1}{N-1}\sum_{i=1}^{N}(x_i - \bar{x})^2} \tag{1}$$

In the above formula, N is the total number of the image's pixels, $\bar{x}$ denotes the mean gray value of the image, and x_i denotes the *ith* pixel's gray value in the image.

According to (1), $\hat{\mu} = 132$ and $\hat{\sigma} = 11$ are calculated as two estimated parameters of Gaussian distribution for fitting the Fig.3(a)'s actual histogram.

In order to better explain that maritime image's histogram obeys Gaussian distribution approximately, the PSNR

(Peak Signal Noise Ratio) between the actual histogram and the fitting Gaussian distribution is proposed in (2), where MSE denotes the Mean Square Error between $h(i)$ and $\hat{h}(i)$, $h(i)$ denotes the actual histogram's pixel frequency, and $\hat{h}(i)$ represents the fitting distribution's pixel frequency, the maximum value of $(h(i) - \hat{h}(i))^2$ is equal to 1, which is put as the numerator of the mathematic expression, the larger PSNR value has, the better the fitting Gaussian distribution approaches to the true histogram.

$$\mathrm{PSNR} = 10 \cdot \lg \frac{1^2}{\mathrm{MSE}} = 10 \cdot \lg \frac{1^2}{\frac{1}{256}\sum_{i=0}^{255}[h(i) - \hat{h}(i)]^2} \tag{2}$$

From Tab. 1, each histogram's PSNR value is more than 40dB, which can reflect that the actual maritime image's histogram is quite similar with the fitting Gaussian distribution.

TABLE 1. The PSNR between the actual histogram and the fitting result (unit:dB).

The number of sub-figure	1	2	3	4
visible maritime image's histogram	54.34	46.12	55.68	44.40
visible color maritime image's histogram	48.29	40.36	46.24	44.99
infrared maritime image's histogram	45.62	51.74	45.03	44.42

III. THE DISCUSSION OF OPTIMAL THRESHOLD SELECTION'S STRATEGY

As we mentioned above, the middle gray-value range occupies the dominated part in the total histogram, thus the total of the frequency in the middle range should be preserved in the process of sub-histogram equalization in order to keep the original image's mean brightness, otherwise it can cause some distortion and artifacts, such as another algorithm's result in the Section V. Three sub-histograms equalization by two thresholds is reasonably designed for enhancing the maritime image, and in this section, the optimal threshold selection's strategy is proposed after the comparison of different enhancement performances caused by different thresholds' selection methods.

A. THE DISCUSSION OF TWO THRESHOLDS' LOCATION SELECTION

Without loss of generality, three different methods on threshold's location selection are discussed as the three following cases (t_1 and t_2 denote the two thresholds respectively):

Case 1: Both of the two thresholds locate on the left side of $\hat{\mu}$, the values of $t_1 = 40$ and $t_2 = 80$ are set as an example for illustration.

Case 2: One threshold locates on the left side of $\hat{\mu}$, and the other threshold locates on the right side of $\hat{\mu}$, the values of $t_1 = 100$ and $t_2 = 170$ are set as an example for illustration.

Case 3: Both of the two thresholds locate on the right side of $\hat{\mu}$, the values of $t_1 = 160$ and $t_2 = 200$ are set as an example for illustration.

We use the image's Mean Brightness (MB) to select the reasonable threshold's direction, in addition, the MB value can be denoted as (3).

$$\mathrm{MB} = \frac{1}{N}\sum_{i=1}^{H}\sum_{j=1}^{W} I(i,j) \tag{3}$$

where N is the total pixel numbers of an image, $I(i, j)$ is the gray value at the *ith* row and the *jth* column of the image's matrix, H is the height of the image's matrix, and W is the width of the image's matrix.

The enhancement result by three sub-histograms equalization under three above-mentioned threshold selection's method is shown in Fig.4, and the MB of the enhancement result with three different cases is shown in Tab. 2. It can be seen that the MB value of Fig.3(a) is 132, if one threshold locates on the left side of $\hat{\mu}$, and the other threshold locates on the right side of $\hat{\mu}$, the MB value after the enhancement result is 135, which can preserve the original image's brightness and produce less noise.

TABLE 2. The MB value of three sub-histograms equalization with two thresholds from three different directions.

Figure number	Fig.3(a)	Fig.4(a)	Fig.4(b)	Fig.4(c)
MB	132	170	135	82

In conclusion, the optimal threshold location selection's strategy is that one threshold locates on the left side of $\hat{\mu}$, and the other threshold locates on the right side of $\hat{\mu}$. Since Gaussian distribution is symmetrical with respect to $\hat{\mu}$, the two thresholds can be set with the same distance towards $\hat{\mu}$, how to select the optimal length is mainly discussed in the following.

B. THE DISCUSSION OF TWO THRESHOLDS' DISTANCE SELECTION

In this section, $\hat{\mu}$ is set as the center, two thresholds with different length centered by $\hat{\mu}$ are discussed, since the maritime image's histogram obeys the Gaussian distribution approximately, $1\hat{\sigma}$ law makes the second sub-histogram have the pixel's proportion of 68.3% approximately, $2\hat{\sigma}$ law makes the second sub-histogram have the pixel's proportion of 95.2% approximately, and $3\hat{\sigma}$ law makes the second sub-histogram have the pixel's proportion of 99.7% approximately, enhancement results under three different laws are shown as Fig.5.

In Fig.5(a) and Fig.5(b), the results under $1\hat{\sigma}$ and $2\hat{\sigma}$ law exist some noise and artifacts in the sea region, thus the performance of $3\hat{\sigma}$ law is more suitable for the maritime

(a) $t_1 = 40$, $t_2 = 80$ (b) $t_1 = 100$, $t_2 = 170$ (c) $t_1 = 160$, $t_2 = 200$

FIGURE 4. Enhancement results by two thresholds from three different directions towards $\bar{\mu}$.

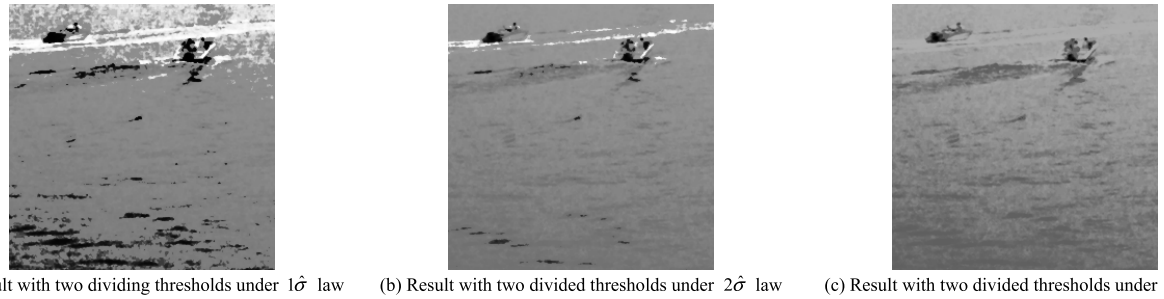

(a) Result with two dividing thresholds under $1\hat{\sigma}$ law (b) Result with two divided thresholds under $2\hat{\sigma}$ law (c) Result with two divided thresholds under $3\hat{\sigma}$ law

FIGURE 5. Enhancement results by two thresholds from three different distances towards $\bar{\mu}$.

image enhancement. The result's histogram after three different laws is shown as Fig.6, from which, it can be seen that $1\hat{\sigma}$ and $2\hat{\sigma}$ law make a certain number of pixels distribute on the first sub-histogram (low gray intensity's range) or the third sub-histogram (high gray intensity's range), by contrast, $3\hat{\sigma}$ law makes only less pixels distribute on the first sub-histogram and the third sub-histogram, a large number of pixels distribute on the second sub-histogram (middle gray intensity's range), thus the enhancement result can suppress the noise and artifacts.

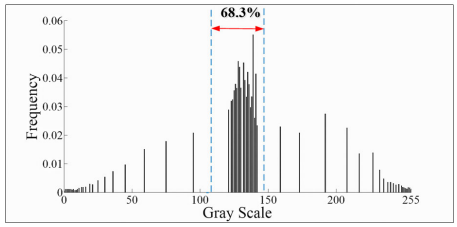

(a) Result's histogram of Fig.5(a)

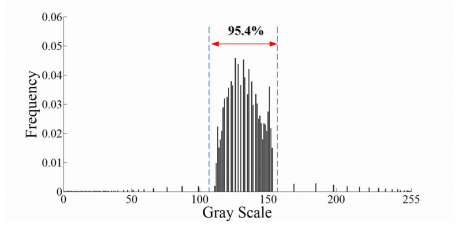

(b) Result's histogram of Fig.5(b)

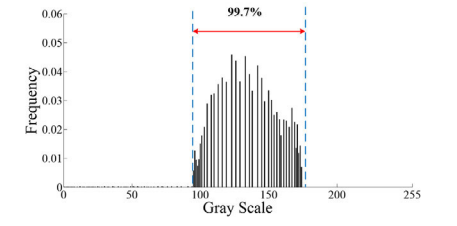

(c) Result's histogram of Fig.5(c)

FIGURE 6. Comparison of result's histogram under three different laws.

IV. THE IMPLEMENT OF TASHE ALGORITHM

The proposed algorithm named by TASHE in this paper can be chiefly described in Tab. 3.

TABLE 3. The chief description of TASHE.

Initialize: Input original maritime image $\boldsymbol{I}$ and define x is the gray value of $\boldsymbol{I}$.
Step1. Calculate $\hat{\mu}$ and $\hat{\sigma}$ derived from the original image according to eq.(1).
Step2. Calculate the adaptive thresholds, divide the original histogram, and obtain the original sub-image.
Step3. Normalize the frequency in the sub-interval, then calculate the $\mathrm{CDF}_1(x)$, $\mathrm{CDF}_2(x)$ and $\mathrm{CDF}_3(x)$ respectively.
Step4. Equalize the three sub-histograms according to the different gray range of x.
End: Output the enhancement result $\boldsymbol{Y}$.

On the adaptive thresholds selection of Step2, according to 3σ law in the statistics, the calculation method proposed for t_1 and t_2 is shown as (4), where k can be chosen under

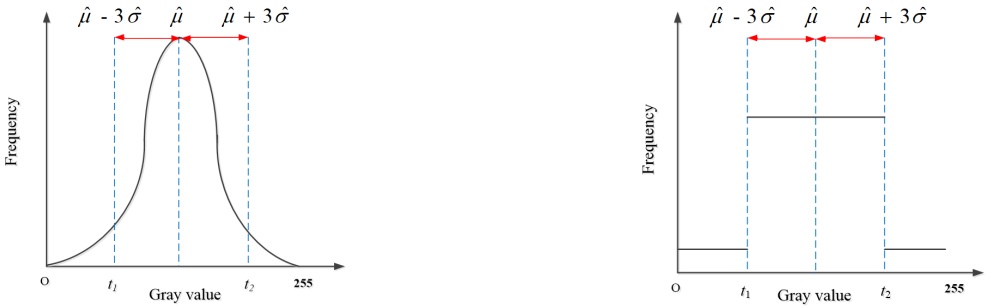

(a) The original image's histogram

(b) The result's histogram after TASHE algorithm

FIGURE 7. Diagram of the histogram's change after TASHE algorithm.

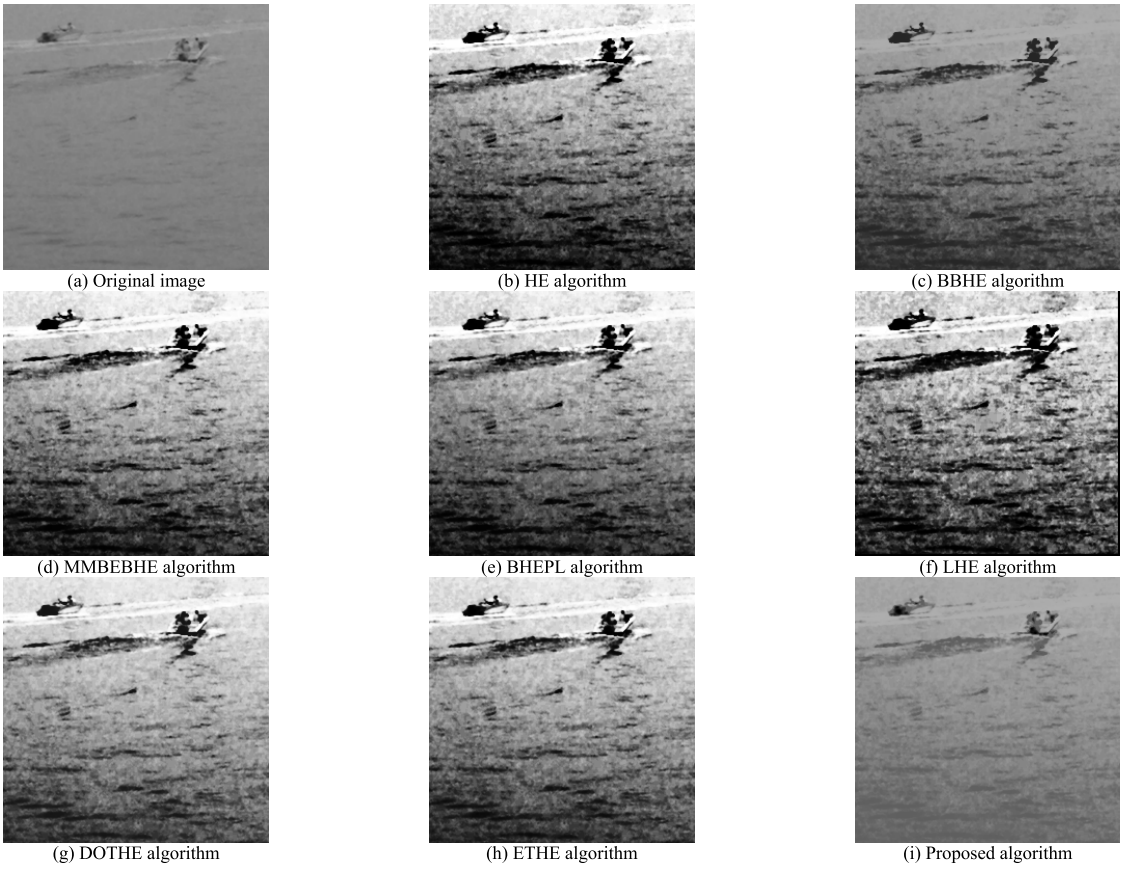

(a) Original image
(b) HE algorithm
(c) BBHE algorithm
(d) MMBEBHE algorithm
(e) BHEPL algorithm
(f) LHE algorithm
(g) DOTHE algorithm
(h) ETHE algorithm
(i) Proposed algorithm

FIGURE 8. Comparison of each algorithm's result for Fig.1(a-1).

the range of [3,5], in this paper, we chose $k = 3$ for the threshold's selection. In some peer researchers' work, LCM (Local Contrast Method) [25] detects the suspected target by the saliency of local contrast, the threshold is also put by the average of local contrast under 3σ law. In the automatic infrared target segmentation's algorithm based on the structure tensor [26], the adaptive threshold for the eigenvalue is selected by the mean value and the standard deviation derived from the statistics of eigenvalue, the main principle is similar with (4).

$$t_1 = \hat{\mu} - k\hat{\sigma}, \quad t_2 = \hat{\mu} + k\hat{\sigma} \tag{4}$$

Since t_1 and t_2 are derived from the original image's histogram, our proposed algorithm is adaptive from different image. In the following, the two thresholds divide the image's total gray range into three sub-intervals, which is shown in (5), correspondingly, three sub-images after sub-histogram equalization can be written as (6) according to the gray range of three sub-intervals.

$$[0, 255] = [0, t_1] \cup (t_1, t_2] \cup (t_2, 255] \tag{5}$$

$$\begin{aligned} \mathbf{X}_1 &= \{\mathbf{I}(i,j);\ 0 \le \mathbf{I}(i,j) \le t_1,\ \forall \mathbf{I}(i,j) \in \mathbf{I}\} \\ \mathbf{X}_2 &= \{\mathbf{I}(i,j);\ t_1 < \mathbf{I}(i,j) \le t_2,\ \forall \mathbf{I}(i,j) \in \mathbf{I}\} \\ \mathbf{X}_3 &= \{\mathbf{I}(i,j);\ t_2 < \mathbf{I}(i,j) \le 255,\ \forall \mathbf{I}(i,j) \in \mathbf{I}\} \end{aligned} \tag{6}$$

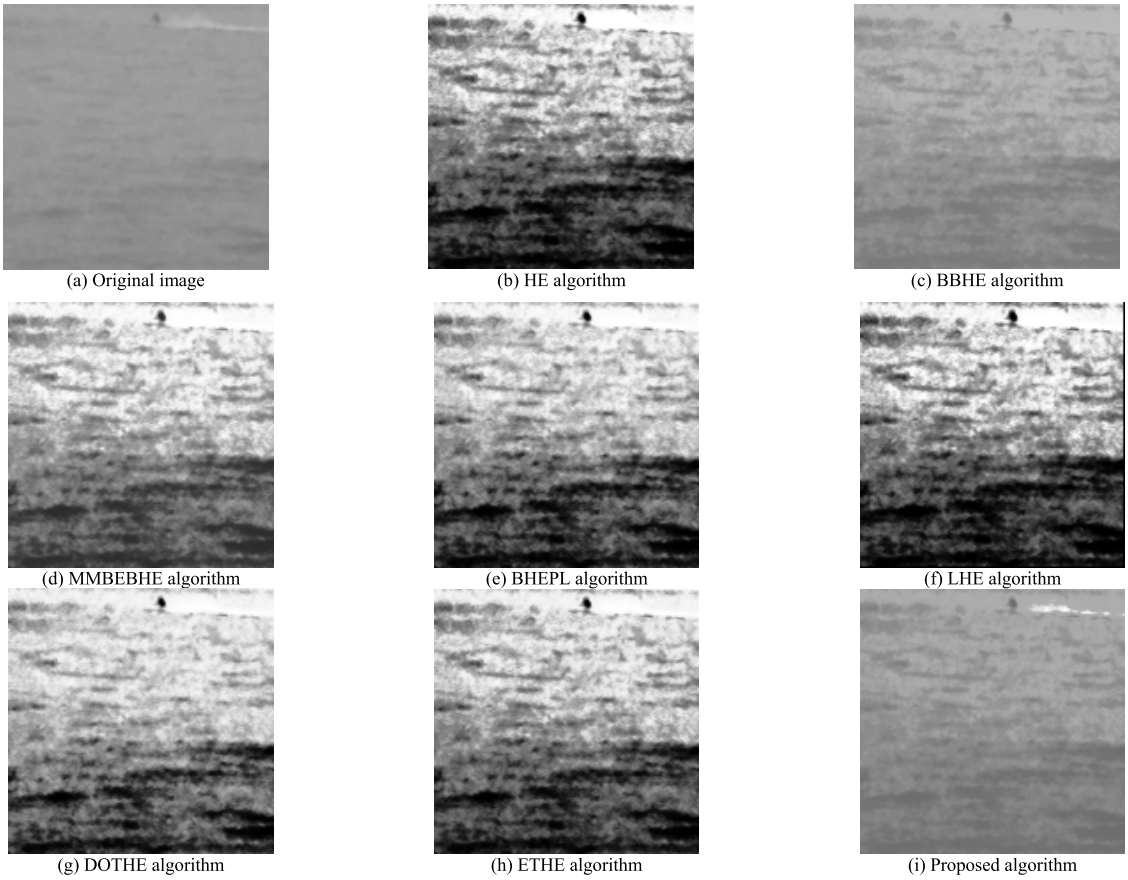

FIGURE 9. Comparison of each algorithm's result for Fig.1(a-2).

where $\boldsymbol{I}$ denotes the original image, $\boldsymbol{I}(i, j)$ represents the gray value whose pixel is in the ith row and the jth column of the image, $\boldsymbol{X}_1$, $\boldsymbol{X}_2$ and $\boldsymbol{X}_3$ denote the first sub-image, the second sub-image, and the last sub-image respectively.

In Step3, we firstly compute each pixel's frequency of the total image and summarize the three sub-histograms' frequency, then the normalized pixel's frequency of each sub-histogram is obtained, finally we need to compute the accumulated normalized frequency of each of three sub-histograms. When x is denoted as the image's gray value, obviously x has three different value's ranges according to eq.(6), when $x \in X_1$, we accumulate the gray level's frequency in the first sub-histogram from 0 to x, the result can be written as $CDF_1(x)$, when $x \in X_2$, we accumulate the gray level's frequency in the second sub-histogram from t_1 to x, the result can be denoted as $CDF_2(x)$, when $x \in X_3$, we accumulate the gray level's frequency in the last sub-histogram from t_2 to x, the result can be denoted as $CDF_3(x)$.

In Step4, we need to compute the transformed gray value after three sub-histograms equalization according to the normalized pixel's frequency of each sub-histogram. First, we use the gray transformation function of traditional HE as a reference to get the sub-histogram equalization's function. The function [23] of gray value's transformation after conventional histogram equalization is described as (7).

$$f(x) = a + (b - a)\,\mathrm{CDF}(x) \tag{7}$$

where a represents the minimum of output's gray value, b represents the maximum of output's gray value, x represents the gray value of the input, $\mathrm{CDF}(x)$ represents the cumulative density function with respect to x. If $a = 0$, $b = 255$, $f(x)$ is the global gray transformation function of conventional HE algorithm. As for three sub-histograms equalization, a, b, and $\mathrm{CDF}(x)$ should be replaced by the reasonable variable of the corresponding sub-interval, thus three sub-histograms equalization can be described as (8).

$$y = \begin{cases} t_1 \mathrm{CDF}_1(x) & if\ x \in [0, t_1] \\ t_1 + 1 + (t_2 - t_1 - 1)\,\mathrm{CDF}_2(x) & if\ x \in (t_1, t_2] \\ t_2 + 1 + (255 - t_2 - 1)\,\mathrm{CDF}_3(x) & if\ x \in (t_2, 255] \end{cases} \tag{8}$$

where y can denote the gray value transformation function in the TASHE algorithm, we can easily get the enhancement result $\boldsymbol{Y}$ by y.

In addition, Fig.7 also shows the histogram's change after TASHE algorithm, it can be indicated that TASHE algorithm equalizes and flattens the three sub-histograms in the three corresponding sub-intervals' gray range.

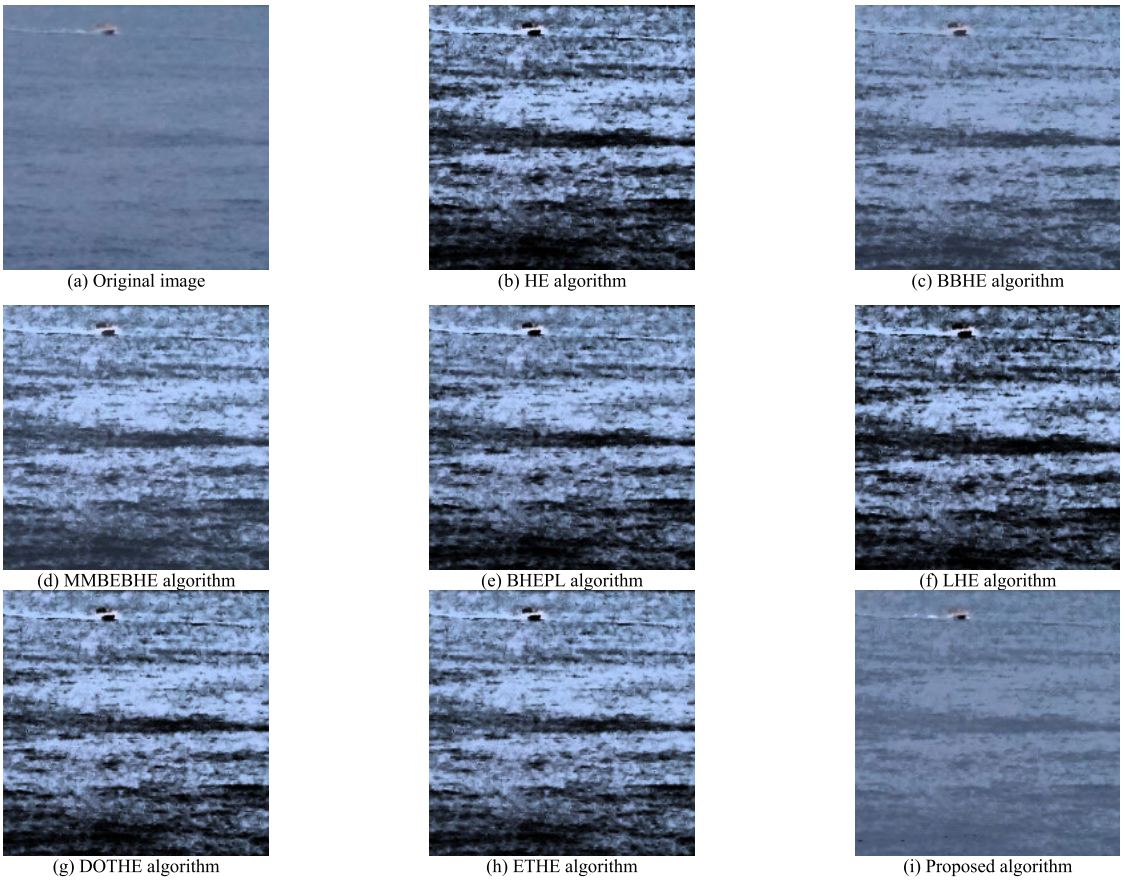

FIGURE 10. Comparison of each algorithm's result for Fig.1(b-1).

V. EXPERIMENTAL RESULTS

In this section, visible gray maritime image, visible color maritime image, and infrared maritime image are chosen to verify the enhancement algorithm's validity. Fig.8(a) and Fig.9(a) are the visible gray maritime images, Fig.10(a) and Fig.11(a) are the visible color maritime images, and Fig.12(a) and Fig.13(a) are the infrared maritime images, which are acquired by a infrared camera in the helicopter above the sea. Meanwhile, we select seven representative modified algorithms based on HE for comparison, the compared algorithms are conventional or novel, the enhancement results are shown in Fig.8, Fig.9, Fig.10, Fig.11, Fig.12 and Fig.13. As for Fig.10(a) and Fig.11(a), we use HSV color space to produce the enhancement result, H component and S component among the HSV color space are kept constant, only V component is processed by each compared algorithm, at last, we transfer the new HSV color space to new RGB color space for displaying the algorithm's result.

The Enhancement Measure by Entropy [24] (EME) and the MB value are used to assess the image's objective quality in Tab. 4, Tab. 5 and Tab. 6. The enhancement result with higher EME value and nearer MB value to the original image has the better enhancement performance.

A. EACH ENHANCEMENT ALGORITHM'S RESULT OF VISIBLE GRAY MARITIME IMAGE

In Fig.8 and Fig.9, HE, MMBEBHE, BHEPL, LHE, DOTHE and ETHE algorithms cause obvious over-enhancement. BBHE algorithm causes some artifacts in Fig.8(c), which is suppressed in Fig.9(c), and the maritime target is enhanced effectively in Fig.9(c), so the performance of BBHE algorithm is not robust. From Tab. 4, it can be seen that the proposed algorithm has the largest EME value, and the MB value of the proposed algorithm is the nearest to the original image's among the compared algorithms, it can be concluded that our proposed algorithm can not only keep the original maritime image's brightness, but also enhance the maritime target. As for some newest algorithms of enhancement for Fig.8(a), the EME values of DOTHE and ETHE algorithm is 1.87 and 1.98 which are lower than the proposed algorithm, and the MB values of these enhancement results are 148 and 140, which have some changes from the original image's.

B. EACH ENHANCEMENT ALGORITHM'S RESULT OF VISIBLE COLOR MARITIME IMAGE

From Fig.10 and Fig.11, it can be seen that HE, BBHE, BHEPL, LHE, DOTHE and ETHE algorithms cause obvious over-enhancement. MMBEBHE algorithm enhances

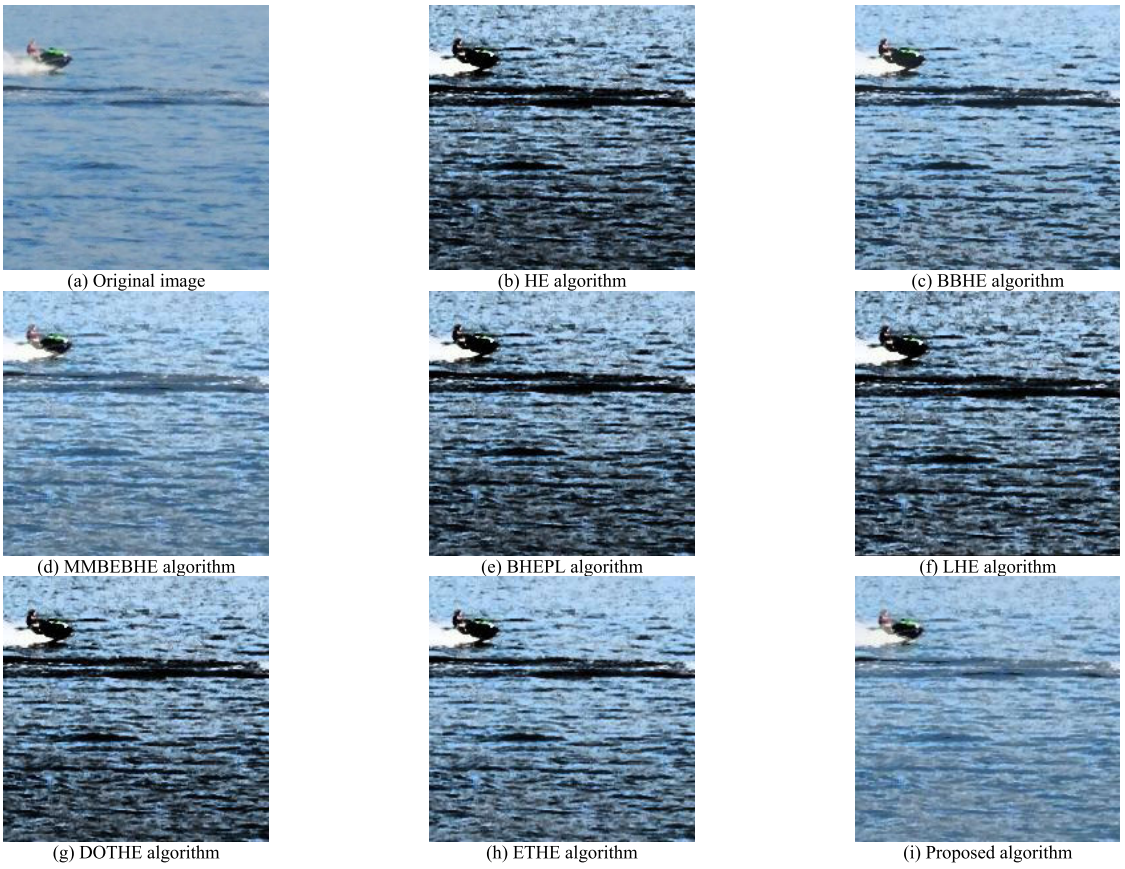

FIGURE 11. Comparison of each algorithm's result for Fig.1(b-3).

TABLE 4. The objective image quality assessment of sub-image in Fig.8 and Fig.9.

Fig.8	Fig.8(a)	Fig.8(b)	Fig.8(c)	Fig.8(d)	Fig.8(e)	Fig.8(f)	Fig.8(g)	Fig.8(h)	Fig.8(i)
EME	0.89	1.24	1.65	1.84	1.87	1.96	1.87	1.98	2.13
MB	132	128	117	136	128	123	148	140	134
Fig.9	Fig.9(a)	Fig.9(b)	Fig.9(c)	Fig.9(d)	Fig.9(e)	Fig.9(f)	Fig.9(g)	Fig.9(h)	Fig.9(i)
EME	0.62	0.78	1.46	1.78	2.05	2.45	2.27	2.39	2.60
MB	149	127	155	154	141	124	153	139	144

the Fig.11(a) effectively, the MB in V component in HSV space of this algorithm's result is 187, which is near to the original image's, and improves the original images to more than 2 times, but it fails to enhance the original maritime image of Fig.10(a), in a word, the performance of MMBEBHE algorithm is not robust, by contrast, the proposed algorithm is more effectively. Tab. 5 is the EME value and the MB value of V component, from Tab. 5, it can be seen that the proposed algorithm's EME value is the largest, and MB value of V component is near to the original image's. In conclusion, the proposed algorithm can also enhance the visible color maritime image effectively.

C. EACH ENHANCEMENT ALGORITHM'S RESULT OF INFRARED MARITIME IMAGE

In Fig.12 and Fig.13, all of the compared algorithms produce heavy distortion in such case, the proposed algorithm keeps the original image's mean brightness and naturalness, and enhances the image's contrast effectively. From Tab. 6, it can be seen that most of the compared algorithms cause serious changes in the original image's MB, by contrast, the proposed algorithm's MB value approaches to the original image's and the EME value is the largest. In a word, the proposed algorithm can also have the enough effectiveness in the infrared maritime image enhancement.

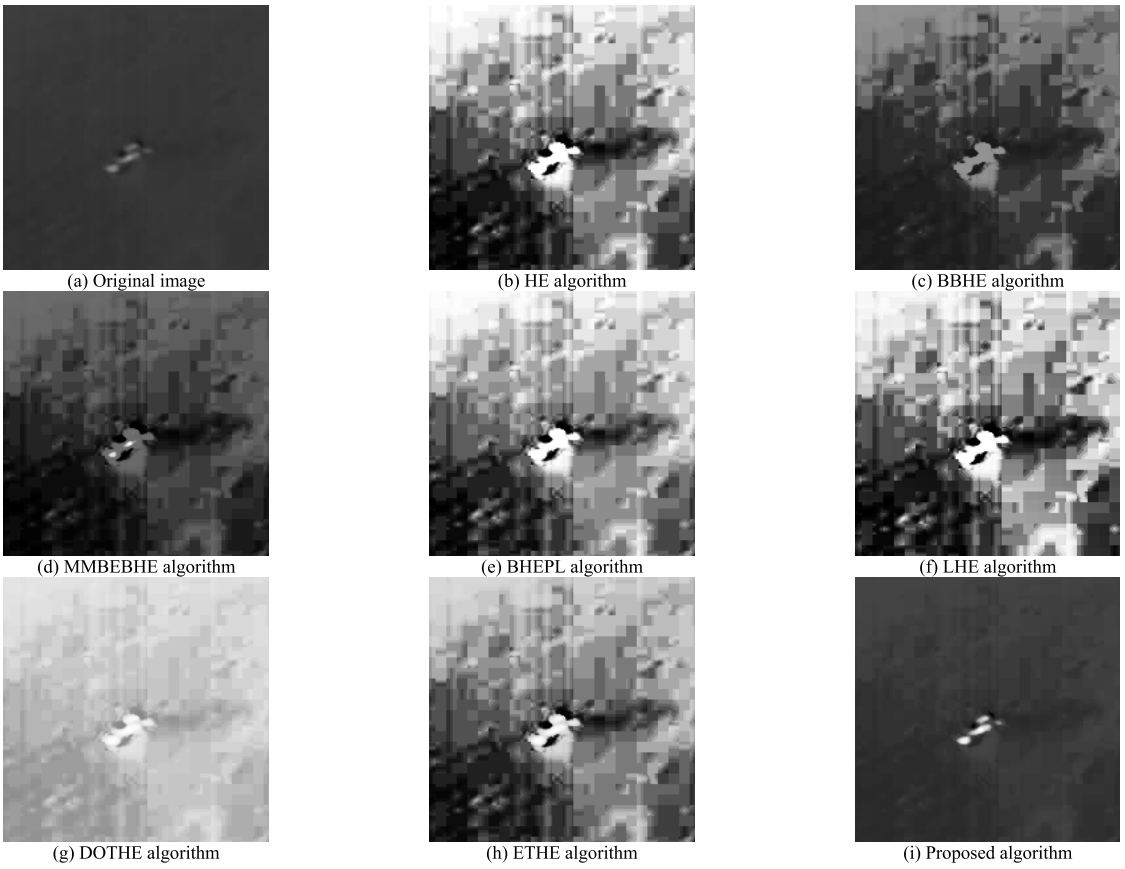

FIGURE 12. Comparison of each algorithm's result for Fig.1(c-1).

TABLE 5. The objective image quality assessment of sub-image in Fig.10 and Fig.11.

Fig.10	Fig.10(a)	Fig.10(b)	Fig.10(c)	Fig.10(d)	Fig.10(e)	Fig.10(f)	Fig.10(g)	Fig.10(h)	Fig.10(i)
EME	1.04	1.15	1.54	2.09	1.87	1.96	2.15	1.98	2.41
MB	156	127	156	164	138	106	142	146	151
Fig.11	Fig.11(a)	Fig.11(b)	Fig.11(c)	Fig.11(d)	Fig.11(e)	Fig.11(f)	Fig.11(g)	Fig.11(h)	Fig.11(i)
EME	1.93	2.64	2.89	4.51	2.97	3.58	3.62	3.87	4.68
MB	185	128	178	187	132	121	136	163	186

TABLE 6. The objective image quality assessment of sub-image in Fig.12 and Fig.13.

Fig.12	Fig.12(a)	Fig.12(b)	Fig.12(c)	Fig.12(d)	Fig.12(e)	Fig.12(f)	Fig.12(g)	Fig.12(h)	Fig.12(i)
EME	0.46	0.58	0.62	0.52	0.82	0.69	0.75	0.87	1.06
MB	54	128	73	59	140	132	194	123	56
Fig.13	Fig.13(a)	Fig.13(b)	Fig.13(c)	Fig.13(d)	Fig.13(e)	Fig.13(f)	Fig.13(g)	Fig.13(h)	Fig.13(i)
EME	0.10	0.19	0.22	0.21	0.24	0.21	0.15	0.14	0.30
MB	105	127	112	117	140	117	74	137	107

In the field of small infrared target's detection, LCM algorithm [25] detects the small or dim target in an infrared image by the saliency of local contrast between the local target's region and local background's region. When the

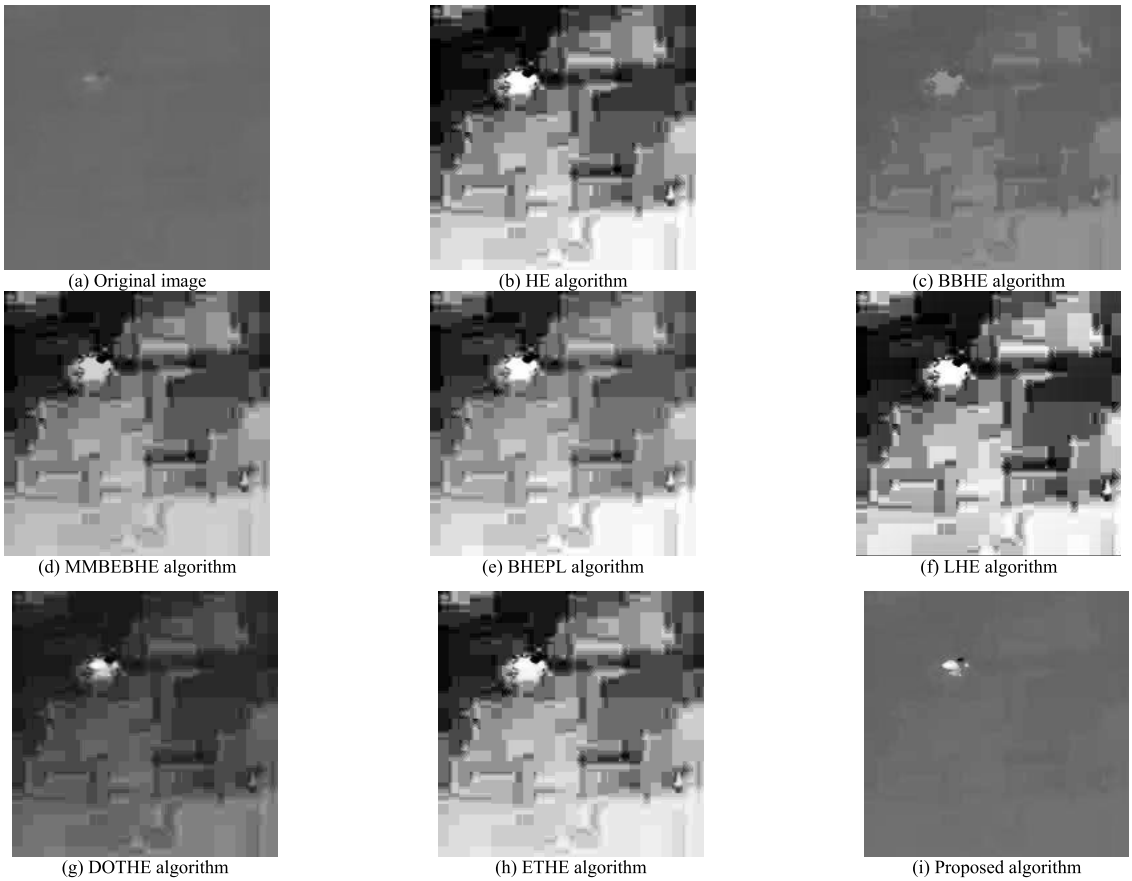

FIGURE 13. Comparison of each algorithm's result for Fig.1(c-2).

maritime image's contrast is increased by enhancing algorithm with less noise and artifacts, the maritime target's Detection Rate (DR) can be increased correspondingly, and the False Alarm Rate (FAR) can be kept in the low level (the calculation for DR and FAR can be referred by [25]), thus our proposed algorithm can be considered as the pre-processing algorithm for the maritime target's detection and tracking. Moreover, in the filed of infrared target's segmentation [26], [27], this proposed algorithm can also improve the segmented target area's accuracy.

VI. CONCLUSION

This paper analyzes the characteristics of maritime image's histogram, and conclude that the histograms of visible gray maritime image, visible color maritime image and infrared image obey the Gaussian distribution nearly, the PSNR between the factual histogram and the fitting curve is more than 40 dB, so Gaussian distribution can be used to fit the histogram of the maritime image. According to the characteristics of Gaussian distribution, three adaptive sub-histograms equalization is designed for maritime image enhancement, the optimal threshold's selection strategy is discussed and the implement of three sub-histograms equalization is described in this paper, the thresholds are derived from the image's histogram, thus the algorithm can be adaptive to different maritime images. From the experimental results, it can be seen that the proposed algorithm keeps the original image's mean brightness, enhances the target effectively, suppresses the sea background's over-enhancement and avoids noise effectively. The objective image quality assessment can also indicate that the proposed algorithm can improve the EME value of the original maritime image, furthermore, the proposed algorithm can also be used as the effective pre-processed algorithm for maritime target's detection and tracking.

In future, we can study the valid algorithm to enhance the sea & sky image, when the image includes sea and sky background, the histogram can be divided by two sub-Gaussian distributions, correspondingly, the effective algorithm based on reformed histogram equalization can also be studied.

REFERENCES

[1] R. Gonzalez and R. Woods, *Digital Image Processing*. Reading, MA, USA: Addison-Wesley, 1992.

[2] P. Kandhway, A. K. Bhandari, and A. Singh, "A novel reformed histogram equalization based medical image contrast enhancement using krill herd optimization," *Biomed. Signal Process. Control*, vol. 56, Feb. 2020, Art. no. 101677.

[3] Sonali, S. Sahu, A. K. Singh, S. P. Ghrera, and M. Elhoseny, "An approach for de-noising and contrast enhancement of retinal fundus image using CLAHE," *Opt. Laser Technol.*, vol. 110, pp. 87–98, Feb. 2019.

[4] H. Singh, A. Kumar, L. K. Balyan, and H. N. Lee, "Optimally sectioned and successively reconstructed histogram sub-equalization based gamma correction for satellite image enhancement," *Multimedia Tools Appl.*, vol. 78, pp. 20431–20463, Mar. 2019.
[5] H. Singh, A. Kumar, L. K. Balyan, and G. K. Singh, "A novel optimally weighted framework of piecewise gamma corrected fractional order masking for satellite image enhancement," *Comput. Electr. Eng.*, vol. 75, pp. 245–261, May 2019.
[6] G. Chen, L. Li, W. Jin, M. Liu, and F. Shi, "Image contrast enhancement method based on display and human visual system characteristics," *Appl. Opt.*, vol. 58, no. 7, pp. 1813–1823, 2019.
[7] M. F. Khan, D. Goyal, and M. Nofal, "Fuzzy-based histogram partitioning for bi-histogram equalization of low contrast images," *IEEE Access*, vol. 8, pp. 11595–11614, 2020.
[8] Y.-T. Kim, "Contrast enhancement using brightness preserving bi-histogram equalization," *IEEE Trans. Consum. Electron.*, vol. 43, no. 1, pp. 1–8, Feb. 1997.
[9] Y. Wang, Q. Chen, and B. Zhang, "Image enhancement based on equal area dualistic sub-image histogram equalization method," *IEEE Trans. Consum. Electron.*, vol. 45, no. 1, pp. 68–75, Feb. 1999.
[10] S.-D. Chen and A. R. Ramli, "Minimum mean brightness error bi-histogram equalization in contrast enhancement," *IEEE Trans. Consum. Electron.*, vol. 49, no. 4, pp. 1310–1319, Nov. 2003.
[11] Q. Wang and R. Ward, "Fast Image/Video contrast enhancement based on weighted thresholded histogram equalization," *IEEE Trans. Consum. Electron.*, vol. 53, no. 2, pp. 757–764, May 2007.
[12] C. Ooi, N. Pik Kong, and H. Ibrahim, "Bi-histogram equalization with a plateau limit for digital image enhancement," *IEEE Trans. Consum. Electron.*, vol. 55, no. 4, pp. 2072–2080, Nov. 2009.
[13] K. Singh and R. Kapoor, "Image enhancement using exposure based sub image histogram equalization," *Pattern Recognit. Lett.*, vol. 36, pp. 10–14, Jan. 2014.
[14] M. Kim and M. Chung, "Recursively separated and weighted histogram equalization for brightness preservation and contrast enhancement," *IEEE Trans. Consum. Electron.*, vol. 54, no. 3, pp. 1389–1397, Aug. 2008.
[15] M. Tiwari, B. Gupta, and M. Shrivastava, "High-speed quantile-based histogram equalisation for brightness preservation and contrast enhancement," *IET Image Process.*, vol. 9, no. 1, pp. 80–89, Jan. 2015.
[16] J.-Y. Kim, L.-S. Kim, and S.-H. Hwang, "An advanced contrast enhancement using partially overlapped sub-block histogram equalization," *IEEE Trans. Circuits Syst. Video Technol.*, vol. 11, no. 4, pp. 475–484, Apr. 2001.
[17] Y. Wang and Z. Pan, "Image contrast enhancement using adjacent-blocks-based modification for local histogram equalization," *Infr. Phys. Technol.*, vol. 86, pp. 59–65, Nov. 2017.
[18] H. Lidong, Z. Wei, W. Jun, and S. Zebin, "Combination of contrast limited adaptive histogram equalisation and discrete wavelet transform for image enhancement," *IET Image Process.*, vol. 9, no. 10, pp. 908–915, Oct. 2015.
[19] K. Singh, D. K. Vishwakarma, G. S. Walia, and R. Kapoor, "Contrast enhancement via texture region based histogram equalization," *J. Mod. Opt.*, vol. 63, no. 15, pp. 1444–1450, Aug. 2016.
[20] M. Song, H. Qu, G. Zhang, S. Tao, and G. Jin, "A variational model for sea image enhancement," *Remote Sens.*, vol. 10, no. 8, p. 1313, Aug. 2018.
[21] T. Celik and T. Tjahjadi, "Automatic image equalization and contrast enhancement using Gaussian mixture modeling," *IEEE Trans. Image Process.*, vol. 21, no. 1, pp. 145–156, Jan. 2012.
[22] C. Ding, L. Dong, and W. Xu, "Image gradient histogram's fitting and calculation," *J. Eng.*, vol. 2018, no. 1, pp. 45–48, Jan. 2018.
[23] E. F. Arriaga-Garcia, R. E. Sanchez-Yanez, J. Ruiz-Pinales, and M. D. G. Garcia-Hernandez, "Adaptive sigmoid function bihistogram equalization for image contrast enhancement," *J. Electron. Imag.*, vol. 24, no. 5, Sep. 2015, Art. no. 053009.
[24] S. S. Agaian, B. Silver, and K. A. Panetta, "Transform coefficient histogram-based image enhancement algorithms using contrast entropy," *IEEE Trans. Image Process.*, vol. 16, no. 3, pp. 741–758, Mar. 2007.
[25] C. L. Philip Chen, H. Li, Y. Wei, T. Xia, and Y. Yan Tang, "A local contrast method for small infrared target detection," *IEEE Trans. Geosci. Remote Sens.*, vol. 52, no. 1, pp. 574–581, Jan. 2014.
[26] Y. Li, Z. Li, Z. Ding, T. Qin, and W. Xiong, "Automatic infrared ship target segmentation based on structure tensor and maximum histogram entropy," *IEEE Access*, vol. 8, pp. 44798–44820, 2020.
[27] X. Ren, J. Wang, T. Ma, C. Yue, and K. Bai, "Adaptive background suppression method based on intelligent optimization for IR small target detection under complex cloud backgrounds," *IEEE Access*, vol. 8, pp. 36930–36947, 2020.

CHANG DING received the Ph.D. degree in information and communication engineering from Dalian Maritime University, Dalian, China, in 2018. He is currently a Lecturer with the school of Mechanical and Electrical Engineering, Guilin University of Electronic Technology. He has published more than ten papers in the international and national journals, and he is also a reviewer for some international and national journals. His research interest includes image enhancement, object's detection and recognition, industrial detection, and machine learning.

XIPENG PAN received the Ph.D. degree from the Beijing University of Posts and Telecommunications, China, in 2019. He is currently an Assistant Researcher with the School of Computer Science and Information Security, Guilin University of Electronic Technology, China. His research interests include machine learning and medical image processing. He has published more than ten papers, and he is a member of CCF and a member of ISAIR.

XINGYU GAO received the Ph.D. degree in measure technology and instrument from Tianjin University, China, in 2010. From 2008 to 2009, he was also a Joint Ph.D. Candidate with Swinburne University, Australia. He is currently a Professor and a Ph.D. Supervisor with the School of Mechanical and Electrical Engineering, Guilin University of Electronic Technology. In addition, he is the Chair of the School of Mechanical and Electrical Engineering, Guilin University of Electronic Technology and the Associated Chair of the Shenzhen Institute on Electronic Information and Advanced Manufacture Technology, Guilin University of Electronic Technology. As for the part-time academic, he is an Associated Chair of Guangxi Mechanical Engineering Society. He has published over 30 papers in some international journals and conferences, and he has directed over ten projects. His current research interest includes industrial detection by computer vision, robot technology, and intelligent manufacturing.

LIHUA NING received the M.S. degree from the Guilin University of Electronic Technology, in 2006. She is currently a Lecturer with the School of Mathematics and Computing Science, Guilin University of Electronic Technology. Her research interests include intelligent calculation and optimization solution.

ZIKU WU received the Ph.D. degree from the Ocean University of China, China, in 2005. He has published more than ten SCI/EI indexed papers. He is currently a Professor with the School of Science and Information, Qingdao Agricultural University. His main research direction is applied mathematics.